# Supplemental Material for Epicardial Fibrosis Explains Increased Endo-Epicardial Dissociation and Epicardial Breakthroughs in Human Atrial Fibrillation

Ali Gharaviri, PhD; Elham Bidar, MD; Mark Potse, PhD; Stef Zeemering, PhD; Sander Verheule, PhD; Simone Pezzuto, PhD; Rolf Krause, PhD; Jos G. Maessen, MD, PhD; Angelo Auricchio, MD, PhD; and Ulrich Schotten, MD, PhD

## S1 Diffuse and patchy fibrosis model

Fibrotic tissue was simulated by randomly assigning the special type "fibrotic" to a given fraction $f$ of model elements. In the diffuse fibrosis model, we simply took a random combination of $\lfloor N\,f \rfloor$ myocardial voxels, where $N$ is the total number of myocardial voxels. We simulated 3 diffuse fibrosis models, with 50%, 70%, and 80% fraction of fibrosis.

Patchy fibrosis models were based on a heterogeneous distribution of the probability of a voxel being selected as "fibrotic". The background probability distribution was a multiscale, spatially-correlated random field (see Figure S1, panel E and F). This random field was obtained with the following steps:

1. Two random Gaussian fields, $g_1(x)$and $g_2(x)$, with squared-exponential, spatial covariance of the form

$$k(x,y) = \exp\left(-\frac{d(x,y)^2}{2\rho^2}\right), \quad x,y \in \Omega, \tag{1}$$

of characteristic length $\rho$ respectively equal to 2 cm and 4mm were generated. The fields $g_1(x)$and $g_2(x)$ account respectively for coarse-scale and fine-scale spatial correlations. The function $d(x,y)$ was the geodetic distance between the points $x$ and y, computed numerically with the Eikonal equation.

2. The random fields $g_1$ and $g_2$ were averaged into a single field $g$:

$$g(x) = \frac{g_1(x) + g_2(x)}{2}.$$

3. The resulting random field was rescaled as follows:

$$h(x,t) = \frac{1}{2}\left(1 + \tanh\left(\frac{g(x)-t}{\varepsilon}\right)\right),$$

with $\varepsilon = 0.2$ and $t \in= [0,1]$.

4. For each voxel of the computational grid, voxel $x$ was fibrotic if $h(x,t) \geq H$, $H \sim \mathcal{U}([0,1])$, with $t$ such that the total number of fibrotic voxels was, on average, equal to the given fraction $f$:

$$\int_{\Omega} h(x,t) = f|\Omega|.$$

The coarse-scale random field $g_1(x)$ was obtained from the truncated Karhuhen -Loève (KL) expansion of the covariance function. The method is outlined by Pezzuto et al. (2018) Briefly, a low-rank approximation of the Hilbert-Schmidt operator

$$\mathcal{K}[\Phi](y) = \int_{\Omega} k(x,y)\Phi(\mathrm{x})d_x,$$

associated to the covariance function (1), was considered. The distance $d(x,y)$ inside the kernel was evaluated with the eikonal equation. Since the correlation function decays slowly, because the correlation length is large, only a few terms in the KL expansion were needed.
The fine-scale random field $g_2(x)$ was sampled through the iterative solution of a stochastic partial differential equation (SPDE) of the following form (Lindgren et al., 2011):

$$(\theta^2 - \Delta)^{\alpha/2}\, u(x) = \mathcal{W}(x),\ x \in \Omega \qquad (2)$$

with $\alpha = v + d/2, v > 0, \theta > 0, \Delta$ the Laplace operator, and $\mathcal{W}$ Gaussian white noise with unit variance. In the model, $d = 3$ (space dimension), and $\kappa^2 = 4v/\rho^2$. With these assumptions, when $v \to \infty$, the solution $u(x)$approximates a random Gaussian field with square-exponential Gaussian correlation with characteristic length $\rho$. The parameter $v$ was set equal to $\frac{4m-3}{2}, m = 1,2, \ldots$, so that the pseudo-differential operator $(\theta^2 - \Delta)^{\alpha/2}$ was the product of $m$ elliptic operators of the form $(\theta^2 - \Delta)$. The problem (2) was eventually solved iteratively as follows:

$$u_0 = \mathcal{W}, \qquad (\theta^2 - \Delta)u_{m+1} = u_m, \qquad m = 1,2, \ldots \qquad (2)$$

An example of diffuse and patchy fibrosis is shown in Figure S1.

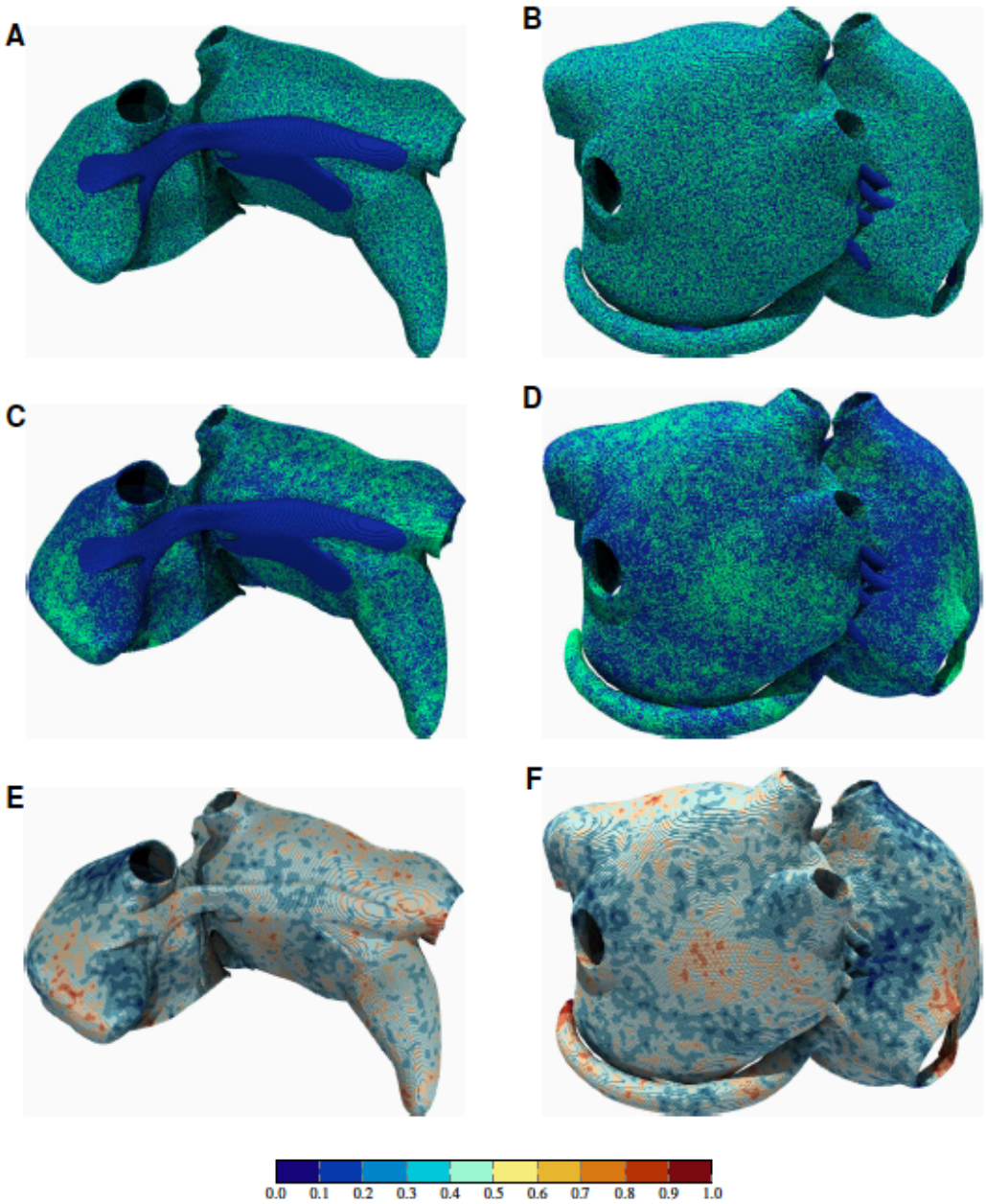


**Figure S1:** Posterior and anterior view of the atria with diffuse and patchy fibrosis. A) Diffuse fibrosis model, 50% fibrotic (anterior view). B) Diffuse fibrosis model, 50% fibrotic (posterior view). C) Patchy fibrosis model, 50% fibrotic (anterior view). D) Patchy fibrosis model, 50% fibrotic (posterior view). E) Background random field for patchy fibrosis (anterior view). F) Background random field for patchy fibrosis (posterior view). Brighter voxels are fibrotic in the model.

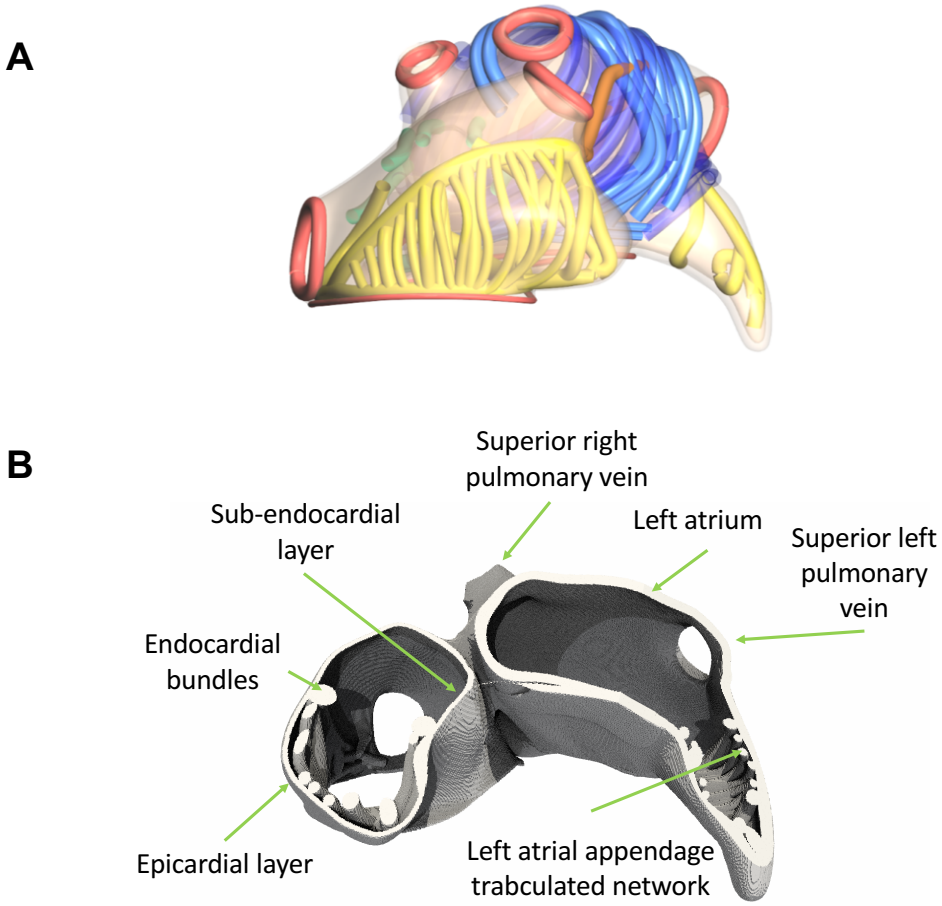


**Figure S2:** A) Geometrical objects created manually. Endocardial bundles are in yellow. Splines used for fiber orientation generations are in Blue and dark blue. B) Cross sectional view of the atrial geometry.

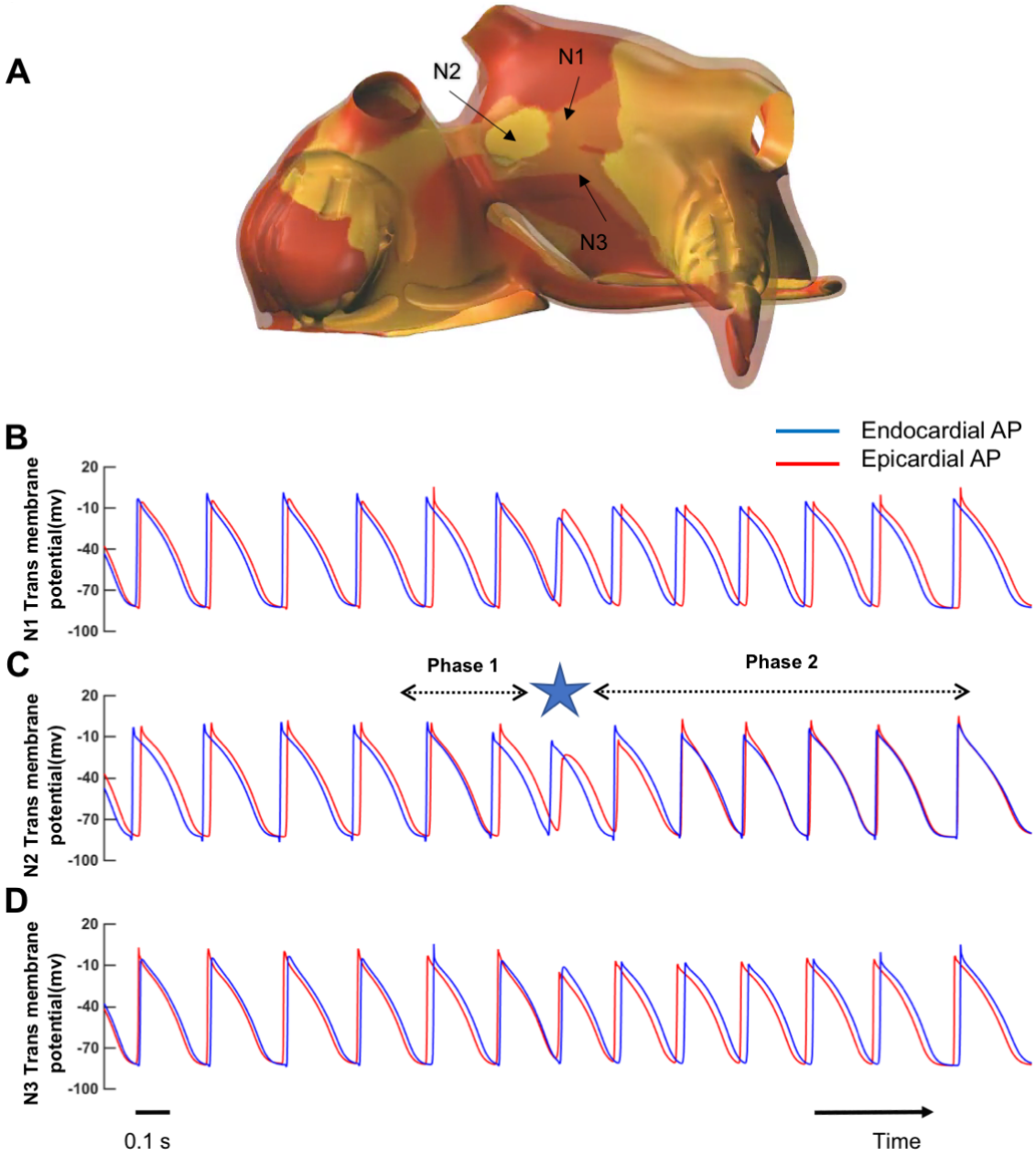


**Figure S3:** Simultaneous endocardial and epicardial simulated action potentials during a breakthrough. A) An example of a breakthrough and the locations of the simultaneous endo-epi APs. B) Simultaneous endo-epi AP at a neighbouring node close to the position of the breakthrough (node N1). C) Simultaneous endo-epicardial APs at the centre of a breakthrough (N2). The star indicates the moment of epicardial breakthrough (node N1). Phase 1 indicates time period in which EED started to increase, leading to a breakthrough. Phase 2 illustrates the disappearance of EED due to the occurrence of the breakthrough. D) Simultaneous endo-epi AP at a node further from the BT position (node N3).

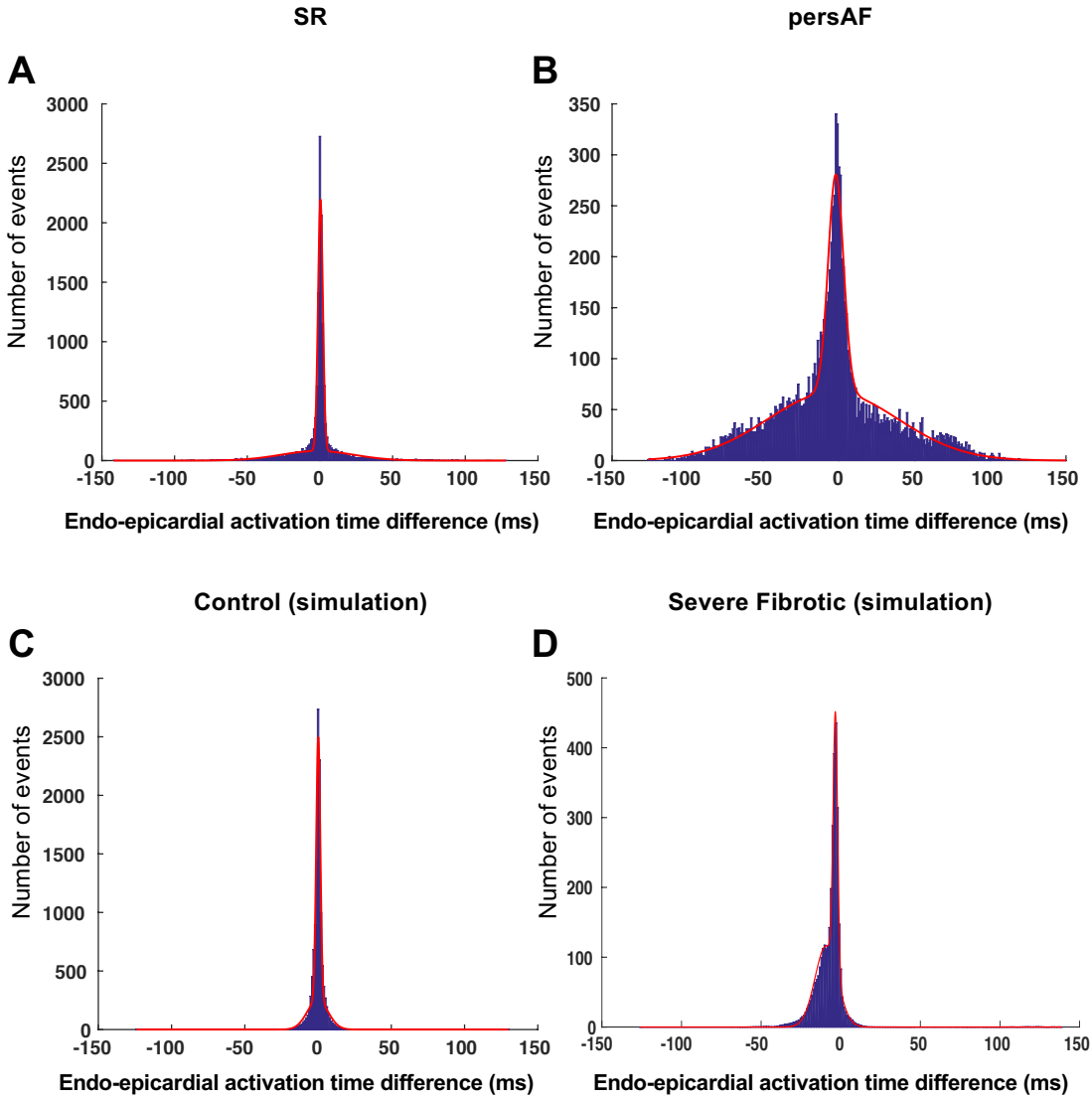


**Figure S4:** Activation time differences between the endo- and epicardial layers in patients (upper panels) and simulations (lower panels). A) Histogram of endo-epicardial activation time differences in A) an SR patient, B) a persAF patient, C) a control simulation and D) a simulation of severe fibrosis. X-axes denotes the difference in activation time (ms) and y-axes denotes the number of events.

**Reference:**

Lindgren, F., Rue, H., and Lindström, J. (2011). An explicit link between Gaussian fields and Gaussian Markov random fields: the stochastic partial differential equation approach. *Journal of the Royal Statistical Society: Series B (Statistical Methodology)* 73(4)**,** 423-498. doi: 10.1111/j.1467-9868.2011.00777.x.

Pezzuto, S., Gharaviri, A., Schotten, U., Potse, M., Conte, G., Caputo, M.L., et al. (2018). Beat-to-beat P-wave morphological variability in patients with paroxysmal atrial fibrillation: an in silico study. *Europace* 20(suppl_3)**,** iii26-iii35. doi: 10.1093/europace/euy227.